

**DESIGN AND EVALUATION OF POLYCARBONATE MICROLENS ARRAYS FOR  
HYBRID CONCENTRATION PHOTOVOLTAIC CELLS**

by

Alyssa Lynn Vessey

A thesis submitted to the Faculty of the University of Delaware in partial fulfillment  
of the requirements for the degree of Master of Science in Electrical and Computer  
Engineering

Fall 2015

Copyright 2015 Alyssa Vessey  
All Rights Reserved

ProQuest Number: 10014940

All rights reserved

INFORMATION TO ALL USERS

The quality of this reproduction is dependent upon the quality of the copy submitted.

In the unlikely event that the author did not send a complete manuscript and there are missing pages, these will be noted. Also, if material had to be removed, a note will indicate the deletion.



ProQuest 10014940

Published by ProQuest LLC (2016). Copyright of the Dissertation is held by the Author.

All rights reserved.

This work is protected against unauthorized copying under Title 17, United States Code  
Microform Edition © ProQuest LLC.

ProQuest LLC.  
789 East Eisenhower Parkway  
P.O. Box 1346  
Ann Arbor, MI 48106 - 1346

**DESIGN AND EVALUATION OF POLYCARBONATE MICROLENS ARRAYS FOR  
HYBRID CONCENTRATION PHOTOVOLTAIC CELLS**

by

Alyssa Lynn Vessey

Approved: \_\_\_\_\_

Michael W. Haney, Ph.D.

Professor in charge of thesis on behalf of the Advisory Committee

Approved: \_\_\_\_\_

Kenneth E. Barner, Ph.D.

Chairperson of the Department of Electrical and Computer Engineering

Approved: \_\_\_\_\_

Babatunde A. Ogunnaike, Ph.D.

Dean of the College of Engineering

Approved: \_\_\_\_\_

Ann L. Ardis, Ph.D.

Vice Provost for Graduate and Professional Education

### **Acknowledgements:**

Michael Haney, PhD for his advice, guidance, and feedback throughout the project and thesis process.

Sandia National Laboratories, for their knowledge and fabrication expertise, without whom physical tests could not have happened

University of Delaware Institute of Energy Conversion, for generously allowing usage of their indoor measurement equipment

Tian Gu, PhD for his leadership, help, and knowledge throughout all stages of the project.

Gautam Agrawal, for his invaluable measurement assistance and company on a cold roof.

This manuscript is dedicated to:

My family, for sticking with me through everything,

The University of Delaware, for the best seven and a half years of my life,

And Ms. Colleen Dougherty, for putting up with me.

## TABLE OF CONTENTS

LIST OF FIGURES .....	vi
ABSTRACT .....	vii
Chapter	
1. INTRODUCTION.....	1
1.1. Photovoltaic Cells .....	1
1.1.1. Solar Radiation .....	2
1.1.1.1. Direct vs. Diffuse Sunlight .....	2
1.1.2. Basic Photovoltaic Cell Design .....	3
1.1.3. Hybrid Photovoltaic Cell Concept .....	5
1.2. Optical Concentration .....	7
1.2.1. Basic Lenses .....	7
1.2.2. Lens Arrays .....	8
2. PREVIOUS WORK .....	10
2.1. Microlens Arrays .....	10
2.1.1. Characterization Methods .....	10
2.1.1.1. Acceptance Angle .....	12
2.1.1.2. Transmission Spectra .....	13
2.2. Earlier Work on Hybrid Photovoltaic Cells and Lens Arrays .....	15

2.2.1.	Measurement Methods .....	16
2.2.2.	Former Research Results .....	17
3.	DESIGN PROCEDURE .....	20
3.1.	LightTools Creation and Simulation .....	20
3.2.	Fabrication and Materials .....	23
4.	DATA AND ANALYSIS .....	25
4.1.	Outdoor Measurements .....	25
4.1.1.	Outdoor Measurement Method .....	26
4.1.2.	Outdoor Measurement Results .....	28
4.2.	Indoor Measurements .....	29
4.2.1.	Spectroscopy and Transmission Spectra .....	30
4.2.1.1.	Spectroscopy Method .....	30
4.2.1.2.	Spectroscopy Results .....	34
4.2.2.	Spot Diagrams .....	35
4.2.2.1.	Spot Diagram Method .....	36
4.2.2.2.	Results .....	37
4.3.	Analysis of Data .....	39
5.	CONCLUSION AND FUTURE WORK .....	41
	REFERENCES .....	43

## LIST OF FIGURES

Figure 1: HPV Concept Diagram .....	6
Figure 2: Example Spot Diagram .....	9
Figure 3: Average encircle energy from spot diagrams .....	17
Figure 4: Bulk spectroscopy results .....	18
Figure 5: Spectrometer setup configurations .....	19
Figure 6: Defining ASTM 1.5G in LightTools .....	21
Figure 7: LightTools optimization window .....	23
Figure 8: An example of iterative lens design in LightTools .....	23
Figure 9: Acceptance angle measurements from 9/12/14 .....	29
Figure 10: Integrating sphere setups .....	31
Figure 11: Absorption, transmission, and reflection percentages for the module tested on 9/25/14 .....	35
Figure 12: Spot diagram example: (left) natural light photograph of abraded lens array, (right) spot diagram of the lens array .....	39

## **ABSTRACT**

The concept and design for a novel integration of microlens arrays and hybrid concentration photovoltaic cells were examined. Designs to increase the collection efficiency of solar cells for both direct and diffuse illumination were created and rigorously simulated. Promising designs were fabricated and tested in both real-world outdoor conditions as well as indoor controlled experiments in order to measure collection efficiency.

## Chapter 1

### INTRODUCTION

Since the dawn of the electrical age, scientists have been searching for new and improved ways to facilitate the generation of electrical power. At first science used chemical batteries pioneered by the likes of Galvani and Volta<sup>1</sup>, then advanced to electromagnetic generation through the work of Faraday<sup>2</sup>. In 1839, Alexandre Becquerel made the discovery of the curious effect known as the photoelectric effect, but it was not until Einstein's *annus mirabilis* that the effect was understood<sup>3</sup>. After his groundbreaking paper on the effect, scientists learned how to capture the power of the sun to generate electrical currents, and since that time a large area of study has been the optimization and improvement of the so-called photovoltaic cell.

#### 1.1 Photovoltaic Cells

As Einstein and Planck theorized, energy is not a continuous quantity but instead measured in discrete intervals, called *quanta*<sup>4</sup>. In particular, Planck noted the now famous relation that the energy of a photon is given in terms of its wavelength via  $E = h\nu$ , where  $h$  is known as Planck's constant.

The basic operating principle of a photovoltaic cell relies on this key insight to understand. In any material, the electrons are separated into different discrete energy levels, with the most energetic level being called the valance band. In a

semiconductor, there exists an additional energy level above the valance band called the conduction band, with spacing between the two bands known as the bandgap. When any photon with energy greater than or equal to the bandgap strikes the semiconductor, there exists a chance that it will be absorbed by the semiconductor and energize a valance electron to the conduction band. From there, the electron is free to flow across the semiconductor, cause a motion of negative charge in its direction and a motion of positive charge in the opposite direction (the so-called “hole” left behind by the electron). A photovoltaic cell uses this effect, collecting solar energy with semiconductors in order to generate a large quantity of electron-hole pairs and an electric current through two attached terminals.

### **1.1.1 Solar Radiation**

Via nuclear processes, the sun produces vast quantities of photons carrying electromagnetic energy into the solar system. The emission spectrum of the sun can be observed to approximate a blackbody radiating at a temperature of about 5800K. A more precise model of the solar emission spectrum is provided by American Society for Testing and Materials (ASTM), whose data approximates the spectrum as viewed from an observer on the ground under the 1976 US Standard Atmosphere model<sup>5</sup>.

#### **1.1.1.1 Direct vs. Diffuse Sunlight**

In outer space, solar panels are a fairly simple proposition: point the solar panel at the sun and collect energy via the photoelectric effect. On the surface of the earth, on

the other hand, the atmosphere distorts the path of the light and complicates the process of gathering energy.

Scientists differentiate light reaching the surface of the earth into two distinct categories. *Direct* sunlight is light that travels unimpeded from the sun to the earth—this is the light that you see when you look directly at the sun. However, not all sunlight travels to the surface of the earth in a direct line. Photons that strike particles in the atmosphere are deflected away from their original path. This sunlight is referred to as *diffuse* sunlight. The practical difference between these is that the angle that direct sunlight makes with the earth's surface is equal to the angle the sun itself is making with the earth, while diffuse sunlight is bent some angle away. The angle at which a photon can strike a photovoltaic cell and still generate an electron-hole pair is referred to as the *acceptance angle* of the cell, and we often calculate this by finding the full-width half-maximum (FWHM) point of the absorbed energy, plotted versus incidence angle.

Sunlight is also sometimes calculated as part of a third category, referred to as *global* sunlight. This light is the sum total of all of the photons striking a given area, and as such is simply equal to the sum of the direct and diffuse radiation.

### **1.1.2 Basic Photovoltaic Cell Design**

As briefly mentioned in section 1.1, a solar cell works by exploiting the bandgap of semiconducting materials. This bandgap is equal to the energy difference between the valence band, where electrons are normally found, and the conduction band,

where they are free to flow as electrical current. Thanks to the photoelectric effect, it is possible for the semiconducting material to absorb photons of energy greater than or equal to the bandgap in order to excite electrons to the conduction band and generate an electrical current.

Naturally, the bandgap is an important determinant of the efficiency of a photovoltaic cell, since only those photons with energy greater than or equal to the bandgap will actually excite electrons and generate current. If a large percentage of the incident photons have energy below the bandgap, the cell will not generate a sufficient amount of electricity for most applications. As a result, the field of *bandgap engineering* strives to develop methods to create photovoltaic cells with bandgaps ideal for given applications. A primary difference among various photovoltaic cells is the material they are made out of: many are made from silicon (Si), which possesses an intrinsic bandgap of about 1.11 eV at room temperature. In addition to silicon, many are made from so-called III-V materials, such as gallium arsenide (GaAs), which possesses an intrinsic bandgap of about 1.424 eV at room temperature. Bandgaps can also be more explicitly engineered by doping semiconductors with various other materials, or by adjusting the operating temperature of the photovoltaic cell itself.

In order to create a controllable current, photovoltaic cells are actually composed of two different semiconductors. These are usually the same base material with different dopants, but other configurations are also possible. One of these materials

is called *p-type* and generates electrons, while the other is called *n-type* and generates holes for those electrons to recombine in. Putting these two materials together creates a *pn-junction*, through which a current can flow. By attaching conductive terminals to each side of the pn-junction, a photovoltaic cell can effectively convert light energy into an electrical current.

### **1.1.3 Hybrid Photovoltaic Cell Concept**

As an improvement to the standard photovoltaic cell implementation, the idea of concentrated photovoltaics (CPV) has been catching on throughout the scientific community and even beginning to see some deployment in real-world scenarios<sup>6,7</sup>. CPV systems rely on optical lenses placed on top of high efficiency photovoltaic cells in order to capture vastly more sunlight than a regular photovoltaic system would.

CPV systems (usually differentiated into LCPV, for “low concentration photovoltaics”, and HCPV, for “high concentration photovoltaics”) have a number of drawbacks. Most notably, because of the requirement for the incident rays to focus on a single point on the photovoltaic cell itself, CPV systems must be pointed directly at the sun at all times, requiring a tracking system for the cells to be mounted on in order to track the sun across the sky during the day. In addition, this naturally means that the CPV system can only collect direct sunlight, as diffuse sunlight will not properly focus onto the concentration spot.

Thus a possible solution was proposed: the so-called hybrid photovoltaic cell (HPVC)<sup>8,9</sup>. The concept is simple: on the surface, it appears in many ways to be simple to a regular CPV system, with an array of microlenses focusing direct sunlight into concentration points on the photovoltaic surface. Unlike other CPV systems, however, the high-concentration photovoltaics underneath the cell are small and arranged above a substrate of lower-concentration photovoltaics, as pictured:

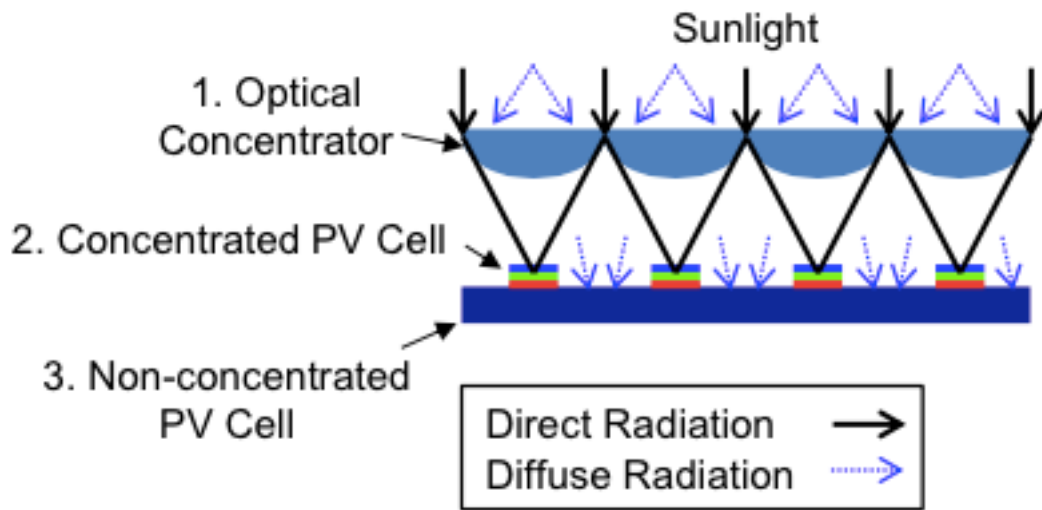


Fig. 1 - HPV Concept Diagram<sup>10</sup>

Because the concentrated PV cells are in the path of focused rays of sunlight, this hybrid system should capture direct sunlight at the same efficiency as a standard CPV system. However, the extra diffuse radiation that is almost entirely wasted in a standard CPV system has a much higher chance of being captured by the non-CPV cells on the lower substrate. While this will not capture all of the diffuse radiation, it will capture vastly more diffuse radiation than a standard CPV would and thus

should prove to be a much more efficient setup for only fractionally more cost and engineering requirement.

## 1.2 Optical Concentration

The principles of optical concentration are largely derived from the basic principles of optics in general, namely Snell's Law and the well-known principles of lens design. Approximating the sun as a 5800K blackbody, the peak intensity is located at a wavelength of around 500nm. Because this wavelength is so small, sufficiently large lenses (say, on the order of millimeters or larger) do not suffer from wavelength-based effects and behave as everyday macroscale lenses.

### 1.2.1 Basic Lenses

We can use the basic laws of lenses to dictate the properties of an optical concentrator, which in the simplest form is merely a circular lens with two curved surfaces on either side. The lensmaker's law<sup>11</sup> states that:

$$\frac{1}{f} = (n - 1) \left( \frac{1}{R_1} - \frac{1}{R_2} \right)$$

In this equation,  $f$  is the focal length,  $n$  is the refractive index (the background index is assumed to be 1), and the  $R$ s are the radius of the front and back side of the lens, respectively. We also use the convention in this equation that for first side of the lens, a convex radius is positive, while for the second side of the lens, a concave radius is positive. In other words, a radius is positive if its lens side is convex when viewed from the incident wave.

Using the definition of the focal length, which states that:

$$\frac{1}{f} = \frac{1}{d_1} + \frac{1}{d_2}$$

In this equation,  $f$  again is the focal length,  $d_1$  is the distance between the source and lens, and  $d_2$  is the distance between the lens and the observing surface. When  $d_1$  is very large, as it is in the case of a solar concentrator, this simplifies to state that  $f = d_2$ . Thus we can find the required distance between any generic lens and solar cell itself through the lensmaker's law.

### 1.2.2 Lens Arrays

A lens array is a set of lenses arranged in a continuous two-dimensional pattern. In the context of concentrated photovoltaics, this array would be placed above a high-concentration solar cell in order to create multiple focal points for sunlight instead of just one. With a lattice spacing of  $a$  between lenses, the spacing between focal points is also equal to  $a$ . Note that this spacing need not be greater than twice the lens radius, and in fact in the case of square patterning a lattice constant of  $a > 2r$  leaves a large space of unfocused radiation between individual lenses in the array. However, in order to maximize the focusing area of the lens array, a hexagonal spacing pattern is vastly superior to a square pattern.

On a basic level, a lens array produces an array of focus spots on the focal surface (the photovoltaic cell, in this case). In a perfectly-manufactured lens array, these

points will be infinitesimally small. Of course, in the real world lenses are never perfectly round or spaced perfectly between each other, so we use a diagram known as a *spot diagram* to detail how well-manufactured the array is.

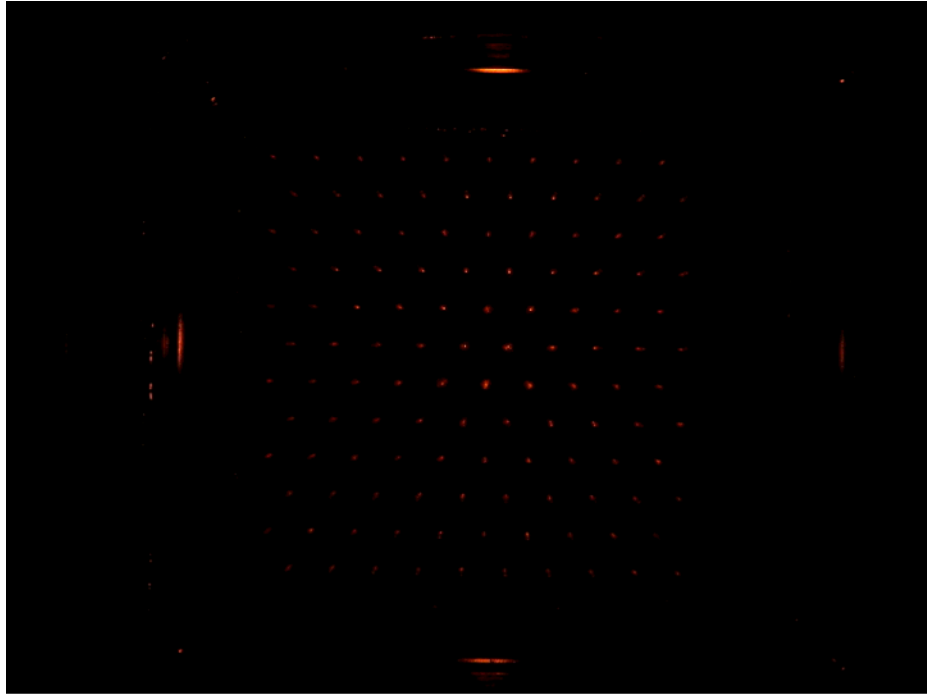


Fig. 2 - Example Spot Diagram (from in-house measurements)

In this example spot diagram, we can observe that certain parts of the focused light appear as *hot spots*, areas where more radiation than desired is focused. These appear as white spots within the larger red spots, especially in the central area of the spot diagram. Note also that the spots appear to be less focused the further from the center we move: this is a drawback of the measurement method, which will be explained in more detail in section 4.2.2.1. In addition, the edges of the sample appear as highly-focused red lines. This is merely a side effect of the finite sample size and should be ignored.

## Chapter 2

### PREVIOUS WORK

Concentrated photovoltaics are not a new concept, nor are the lens arrays often used to focus sunlight onto the cells. As with any research into a scientific field, it is important to keep an eye on past research in order to get an idea of what needs improvement and where further developments can be made. With that in mind, the following is a look at the history of both microlens arrays and concentrated photovoltaics, as well as at previous work on this particular project.

#### 2.1 Microlens Arrays

The work presented in this paper began with a talk at a conference in 2012 presented by Gregory Nielson *et al* at SPIE, the international society for optics and photonics. In the talk, detailed in an invited paper available through SPIE<sup>12</sup>, Nielson describes a theoretical system involving either a silicon or III-V CPV cell as well as a three-stage lens array design for solar collimation and collection. Because of the small size, this system has a number of advantages over a larger CPV system, namely the lower cost to design a mechanical tracking system as well as greatly improved efficiency thanks to the more practical refractive microlenses versus larger macroscale Fresnel lenses, as are often used in large-scale systems.

##### 2.1.1 Characterization Methods

A microlens array design lives or dies by its ability to capture a sufficient percentage of incident sunlight and to focus it with sufficient accuracy on the CPV surface

underneath. To do this we need to define measures by which to characterize a microlens before we can discuss its merits or drawbacks.

The first of these measures is the *acceptance angle*, which describes at what angle from the normal a ray of sunlight may have and still be absorbed by the photovoltaic cell underneath the array. Naturally, this is partly dependent on the cell itself in addition to the microlens array above it. In general, this acceptance angle is defined in full-width half-max (FWHM), meaning that the angle given is the angle at which the absorbed intensity is equal to  $\frac{1}{2}$  that of the maximum intensity, usually assumed to occur at  $0^\circ$ .

A second measure of importance is the *acceptance spectrum*, which as a whole describes the spectrum of light absorbed by the photovoltaic cell. When compared to the solar emission spectrum, the acceptance spectrum can provide valuable insight about the particular wavelengths of light that are or are not being absorbed by the device. This spectrum is dependent both on the qualities of the photovoltaic cell as well as the *transmission spectrum* of the microlens array, which describes the transmission ratio, usually given as a percentage, versus the wavelength at which that transmission is observed. The acceptance spectrum of the device is often condensed into a single number, which again is a FWHM measure of the spectrum, and is used to help quantify the percentage of incident sunlight that will actually be absorbed by the device.

### **2.1.1.1 Acceptance Angle**

The acceptance angle of a concentrating solar harvesting system is a measure used to determine at what angle from the normal a photon can strike the system and still cause the generation of an electron-hole pair in the photovoltaic cell. This is usually expressed in one of two ways, either as a full spectrum of data providing many data points of transmitted intensity vs. incident intensity over some angle range, or as a FWHM figure derived from this data and used as a summary of the system's acceptance characteristics.

It is worth noting that in a concentrated PV system, the acceptance angle is often smaller than in a standard non-concentrating PV system. This is doubly true for systems with concentrating lenses on a layer above the PV cells themselves, since small deviations of the incident angle before the lens are often made larger by the lens itself. However, while a CPV system may have a smaller acceptance angle, the peak intensity as measured at a normal incidence angle is often far greater than it would be on a competing standard PV system. To accommodate the loss in acceptance angle, most CPV systems are mounted on solar tracking systems, to ensure that the maximum amount of sunlight possible is directly incident on the solar cell.

To measure acceptance angle, we used a test photovoltaic cell on top of which we attached a concentrating lens array. These were mounted on top of a tilting stage on a solar tracker rated to  $\pm 0.01^\circ$  accuracy to normal incidence. Data were collected

from the solar cell and could be compared to measurements from a direct solar radiation meter and a global radiation meter, in order to determine what fraction of incident light was being absorbed by the full PV system. Specific acceptance angle measurements were performed by adjusting the tilt of the mounting stage at regular intervals and measuring for about 2-3 minutes. Repeated many times over a single day, these measurements provide a large spectrum of data and the ability to plot the transmitted intensity over angle from normal. A sample of this data has been provided in the appendices and will be discussed in further detail in section 4.1.

#### **2.1.1.2 Transmission Spectra**

Like the acceptance angle, the transmission spectrum of a given concentrating lens array can be expressed either as a full spectrum of data or as a FWHM summary of that data. Unlike the acceptance angle, however, the transmission spectrum is instead a measurement of the total transmitted intensity as measured against the wavelength of the incident photon, rather than the angle of incidence. This is largely a product of the material used to create the lens array, although also depends largely on the design of the PV cell itself.

To measure the transmission spectrum of a given sample, we used an on-site spectrometer capable of generating light rays over a wide spectrum of wavelengths. The sample was placed inside the spectrometer's measurement chamber and analyzed over a range of 300-2000nm wavelengths. Both the transmission and reflection spectra were observed, the reflection spectrum being a similar measure

that instead gives the fraction of incident radiation being reflected off of the lens array instead of transmitted through it. Using these two spectra, the absorption spectrum can also be found, as it is simply equal to the total incident intensity minus both the transmission and absorption spectra.

Note that unlike the acceptance angle measurements, the transmission spectrum does not have an intuitive point at which maximum acceptance is desired. This is because the sun itself does not produce perfect white light, but instead itself has a radiation spectrum that defines how much energy is produced at any given wavelength. According to NREL's US Standard Atmosphere model, peak solar radiation as measured on the ground in the United States occurs somewhere around 500nm. As a result, a desired transmission spectrum of a concentrating lens array allows maximum transmission at around this same point in order to take advantage of the sun's increased energy output at that wavelength.

Finally, because of the spectrometer's design, some hand cleanup of data was necessary. This will be discussed in more detail in section 4.2, but in brief: different subspectra of the overall measurement spectrum are produced by different bulbs, each of which is manufactured in a different way. When a desired wavelength is near the intersection of two different bulb spectra, the physical differences of the two light generation techniques for each bulb become more readily apparent, creating additional noise as one bulb switches off and the next switches on. While the spectrometer has a built-in system for correcting for this error, it is imperfect

and some data must be estimated in order to prevent nonsense data from ruining the overall spectral measurements.

## 2.2 Earlier Work on Hybrid Photovoltaic Cells and Lens Arrays

Work on this project at the University of Delaware began several years before I joined the project. The beginning work was detailed in the paper “Hybrid Micro-scale CPV/PV Architecture” by Michael W. Haney, Tian Gu, and Gautam Agrawal<sup>13</sup>. Further work includes “216 Cell Microconcentrator Module...”<sup>14</sup> and “Performance Characterization of a Small Form-Factor 100X Micro-Optic Concentrator”<sup>15</sup>.

In “Hybrid Micro-scale CPV/PV Architecture”, Michael W. Haney *et al* detail what would become the HCPV system. In particular, the paper details how a hybrid system can theoretically improve upon a basic CPV system thanks to its observation that the efficiency of a hybrid system is given by:

$$\eta_{\text{hybrid}} = T_{\text{conc}} \times \eta_{\text{conc}} \times P_{\text{dir}} + T_{\text{non-conc}} \times \eta_{\text{non-conc}} \times (1 - P_{\text{dir}})$$

In this equation,  $T_{\text{conc}}$  and  $T_{\text{non-conc}}$  are the transmissions onto the concentrated and non-concentrated photovoltaic cells respectively,  $\eta_{\text{conc}}$  and  $\eta_{\text{non-conc}}$  are the quantum efficiencies of the concentrated and non-concentrated photovoltaic cells respectively, and  $P_{\text{dir}}$  is the ratio of direct solar emission to global solar emission.

For a system with a large silicon base photovoltaic cell on top of which a concentrated cell was placed, it was found that the energy improvement factor compared to a standard CPV system is given by:

$$M = 1 + P_{dir} \left( \frac{\eta_{conc}}{\eta_{Si}} - 1 \right)$$

As in the previous equation,  $\eta_{conc}$  and  $\eta_{Si}$  are the quantum efficiencies of the concentrated PV cell and the silicon PV cell respectively (here given as 18% for the silicon cell and 30% for the concentrated cell), and  $P_{dir}$  is the ratio of direct solar emission to global emission, which ranges somewhere between  $\sim 0.6$  and  $\sim 0.8$  throughout the USA. Using this data, the improvement factor was calculated to be somewhere between 1.4 and 1.53 compared to a standard CPV system.

### **2.2.1 Measurement Methods**

For the most part, data collected in the early stages of the project were entirely done via computer simulation software—in particular, the LightTools software package from Synopsys Optical Solutions. As discussed in earlier sections, simulated sources followed the NREL AM1.5D optical spectrum in order to replicate solar emission as closely as possible. These simulation methods allowed rapid prototype and problem-solving during the early stages of microlens array development.

Physical microlens arrays modules were created off-site at Sandia National Laboratories in Albuquerque, New Mexico, then shipped to the University of

Delaware’s main campus in Newark, Delaware for analysis. Modules such as the one described in G. Agrawal’s “Performance Characterization of a Small Form-Factor 100X Micro-Optic Concentrator” were tested in three methods: via a bulk spectrometer to measure the transmission spectrum of the module, via a solar simulator with transmission measured relative to a solar cell without the module, and via a spot transmission set-up in a darkroom. All three of these methods were further used in the more recent research and will be discussed in full in Chapter 4.

### 2.2.2 Former Research Results

The most recent results prior to my introduction to the project were presented in the paper “Performance Characterization of a Small Form-Factor 100X Micro-Optic Concentrator”, whose results are presented below. Overall air-optics-air transmission was found to be ~87%, and the focused transmission in an air-optics-air setup was found to be ~76%. The level of focus can be gleaned from the encircled energy diagram presented in the paper:

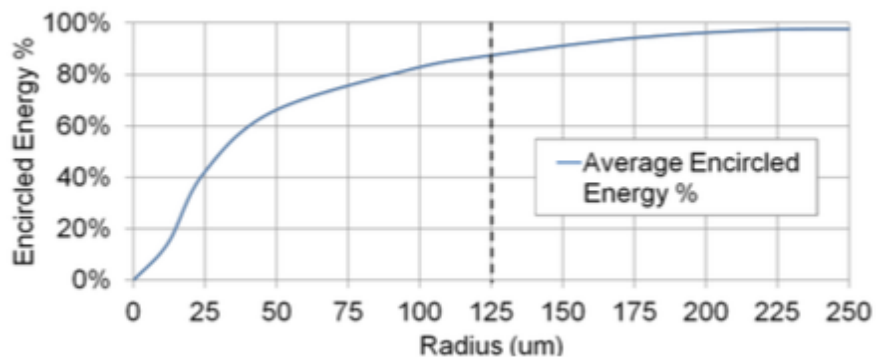


Figure 3 - Average encircled energy from spot diagrams<sup>16</sup>

At the desired focal radius of  $125\mu\text{m}$ , the average encircled energy was found to be 87.45% of the transmitted energy, while in a simulation the same radius gave an encircled energy ratio of 99.1%. The paper's authors attributed these losses to two factors, namely physical limits for accuracy from the mold fabrication as well as errors and scratches on the lens itself.

Similarly, the paper reported bulk spectroscopy measurements in order to show the transmission spectrum of the sample. This figure is reproduced below:

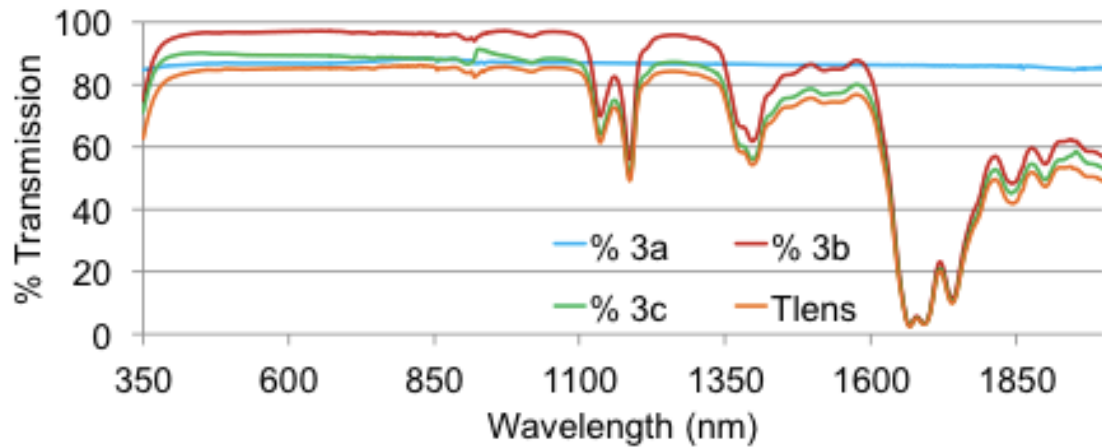


Figure 4 - Bulk spectroscopy results<sup>17</sup>

In this diagram,  $T_{\text{lens}}$  is the bulk transmission of the microlens array, while %3a, %3b, and %3c are all measurements based on certain configurations of the spectrometer and its integrating sphere, as shown below. This will be discussed in more detail in section 4.2.1.1, but for convenience's sake the relevant diagram is reproduced below:

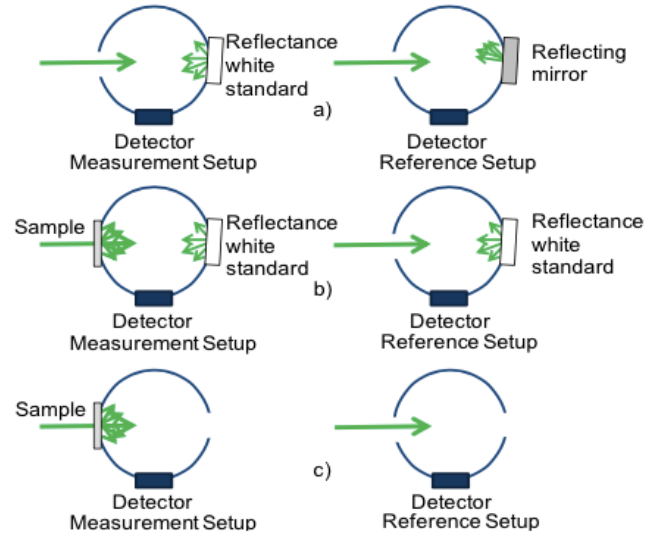


Figure 5 - Spectrometer setup configurations<sup>18</sup>

These three quantities,  $\sigma_{3a}$ ,  $\sigma_{3b}$ , and  $\sigma_{3c}$ , can be found mathematically via the following equations:

$$\sigma_{3a} = \frac{P_{in} \eta_{r-diff}}{P_{in}}$$

$$\sigma_{3b} = \frac{P_{in} T_{lens} (n_{lens-r-diff} \eta_{r-diff} + 1 - n_{lens-r-diff})}{P_{in} \eta_{r-diff}}$$

$$\sigma_{3c} = \frac{P_{in} T_{lens} (1 - n_{lens-r-diff})}{P_{in} \eta_{r-diff}}$$

In these equations,

$P_{in}$  is the source incident power

$\eta_{r-diff}$  is the collected light reflected from rear diffuser

$n_{lens-r-diff}$  is the fraction of incident light incident on the rear diffuser

$T_{lens}$  is the bulk transmission of the array

## Chapter 3

### DESIGN PROCEDURE

During this project, many different iterations of concentrator arrays were designed, manufactured, and tested. Most variations on the array were small adjustments, made to account for small errors found in the previous iteration. The general design procedure was as follows:

1. Generate lens model in the LightTools software package and run simulations to test viability;
2. Once a good model is found, submit to colleagues at Sandia National Laboratories for fabrication;
3. Receive fabricated lens array;
4. Run tests on physical lens array, and compare data to older variations;
5. Propose new changes to the design;
6. Return to step 1 for a new, updated lens array design.

The two primary design components of this process are steps 1 and 2, where both changes to the array as well as new practical considerations must be taken into consideration.

#### 3.1 LightTools Creation and Simulation

Most computer-aided design (CAD) work on this project was performed with LightTools, a simulation and design package available via Synopsis Optical Solutions<sup>19</sup>. LightTools contains a simple drawing interface for producing three-dimensional shapes, light sources, photodetectors, and so on. It also allows the

ability to assign material definitions from a large list of materials, or the ability to custom define material behavior.

The first step, naturally, is to define the light source that will illuminate the model. LightTools allows the definition of custom light sources, meaning that solar emission can be adequately represented by importing the ASTM 1.5G solar model. In addition, the source can be defined with an aim sphere in which light will be emitted, meaning that both direct and diffuse light can be modeled with the software package. The aim sphere is a LightTools setting allowing the simulator to cast rays at random angles within a spherical sector defined by the user.

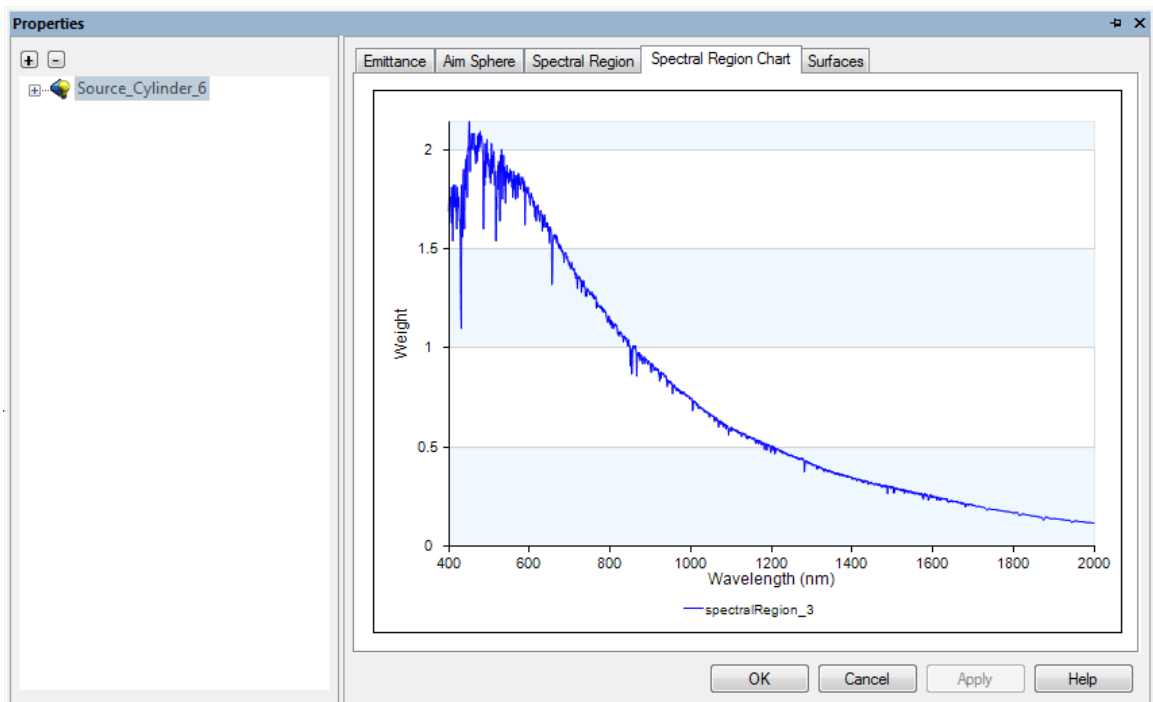


Figure 6 - Defining ASTM 1.5G in LightTools

After the spectrum is defined, it is very easy to produce a source with LightTools.

For the purposes of this research, I used a planar light source emanating in the  $+z$

direction with the above emission spectrum. LightTools allows random variance in the aim sphere of the source, which was often used for simulation after the lens was designed.

Once the source is defined, a receiver is also defined. Receivers allow measurements of multiple different quantities, such as the received intensity, and can measure over a number of variables such as physical  $(x, y)$  coordinates as well as received angle. For the purposes of this experiment, the receivers represent the surface of the photovoltaic cell and were assume to be perfect light absorbers. Obviously this assumption is not true, but it simplifies the process of developing a lens.

Finally, LightTools allows the definition of lenses from a wide array of pre-defined lens materials as well as user-defined materials. In addition, the package allows the definition of both optimization variables and constraints, as well as merit functions and targets. Once the optimization parameters are set, LightTools can perform iterative searches with a number of different algorithms to find a lens that best fits the desired parameters and requirements.



Laboratories in Albuquerque, New Mexico. There the lens arrays fabrication process took place (which involved an outside injection molding vendor) before being shipped back to the University of Delaware to be field-tested under a northeast US atmosphere.

The lens arrays were structured as a sandwich, with polycarbonate on the outside and a PDMS filling inside. Usually, two arrays were made for each model: one with a glass shield and anti-reflection coating to be used for outdoor tests, and another with a scored back surface to be used for indoor tests. While the scored surface naturally harms the transmission of the lens, it allows light to gather on the back surface enough to be observed and photographed. In particular, these modules were useful for producing spot diagrams such as Figure 2.

## Chapter 4

### DATA AND ANALYSIS

After receipt of lens arrays from Sandia, the team at the University of Delaware subjected lens arrays to a number of tests both indoors and outdoors. The collective purposes of all of these tests was to analyze the performance characteristics of the lens arrays in order to learn the ways in which a given generation was working well and the ways in which it could be improved. Once a series of tests was performed on a given generation, we would discuss the results, propose improvements, and return to the design phase with our new goals in mind.

#### 4.1 Outdoor Measurements

While ideally all tests for a given generation of lens arrays would be done outdoors as the target usage is for outdoor power-generating solar panels, this was not always possible for a number of reasons. In order to generate reliable and consistent data despite fluctuations in atmospheric conditions and time of day, a solar tracker was necessary for data collection outdoors. This tracker, while accurate in pointing directly at the sun to  $\pm 0.01^\circ$ , requires perfectly clear skies as it cannot otherwise find the sun. As a result, outdoor measurements could only be done on cloudless days. Even with perfect outdoor conditions, all measurements taken outdoors are still reliant on unknown fluctuations in atmospheric conditions and can change based on the time of day the measurements were taken, meaning that only the most basic information could be gleaned from this procedure--namely, the measurement of the acceptance angle for a given lens array. Despite these issues, the acceptance

angle measurements performed outdoors at the University of Delaware provided valuable information about the performance of each generation of lens array and was an invaluable part of the testing phase for this research.

#### **4.1.1 Outdoor Measurement Method**

Outdoor measurements of the lens arrays were performed atop DuPont Hall at the University of Delaware, which stands three stories above a parking lot. This site was chosen both for its convenience to the research lab across the parking lot as well as its relative isolation compared to other buildings. At no time except very early dawn and very late dusk is the roof covered with shadows, making it a near-ideal location for performing measurements over the course of a day or two.

To perform the measurements, a test solar cell with known performance characteristics was mounted onto a solar tracker capable of  $\pm 0.01^\circ$  sun-tracking accuracy, and then the array to be tested was mounted above this cell. In addition, the solar tracker had secondary solar cells for measuring both the direct sunlight and global sunlight, allowing us to compare the energy collected under the lens array with the available power that was radiating at any given time. This allowed us to accurately account for both the changing received light at various times in the day, as well as random atmospheric fluctuations.

Outdoor measurements were used to test the acceptance angle of the lens array. Since the solar tracker was guaranteed to be pointing close to directly at the sun, we

mounted a two-axis manual stage onto the tracker, upon which the solar cell and lens array were mounted. This allowed tight control of the angle that the solar cell normal was making to the sun.

Once the solar tracker setup was complete, it was time to begin measuring. Because the two-axis stages were manual, I remained on the roof of the building during the day to make gradual adjustments during the acceptance angle testing as follows. After taking a few minutes of measurement with the stages pointed directly at the sun, one stage would be rotated by 10 minutes of arc and measured again for 2-3 more minutes. Each angle and the times of data collection were marked by hand in a notebook to enable us to properly analyze the data and associate each data point with the correct angle, since the data were collected as amperage over time. Since the current generated by a solar cell is directly proportional to the intensity over the cell's operating range, this was equivalent to measuring the capture ratio when compared to the control cell. For both the  $x$ - and  $y$ -axes, the stages would be adjusted by 10 minutes of arc for the first  $\pm 3^\circ$  off of normal, followed by adjustments of 30 minutes of arc until an angle of  $\pm 5^\circ$  off normal. Once one axis was completed, the stages would be reoriented to normal and the other axis would be measured.

After the day's measurements were done, the data were downloaded and analyzed. Each angle measured was correlated to the time marked in the notebook, and then the middle minute of that data was used. The data between both the test cell under

the lens array and the reference cells were averaged over the time and then divided into each other to calculate the fractional quantity of absorbed energy compared to the amount of energy available during that minute. From these data we could produce highly accurate acceptance angle charts and learn how well the lens array captured diffuse light compared to a standard solar cell without a lens array.

#### **4.1.2 Outdoor Measurement Results**

While the overall results were mixed between different lens arrays, there was a clear standout lens array that performed better than any other. This one was tested on September 12, 2014 on top of DuPont Hall at the University of Delaware.

The tests revealed an extremely efficient lens array, with an acceptance angle for 90% intensity of about  $\pm 2.5^\circ$  from normal, and a FWHM of about  $\pm 3.5^\circ$  from normal. At normal incidence fully 46% of global incident light was captured as power, while at  $\pm 5^\circ$  from normal as much as 12% of global incident light was captured. Figure 9 shows the results of these measurements.

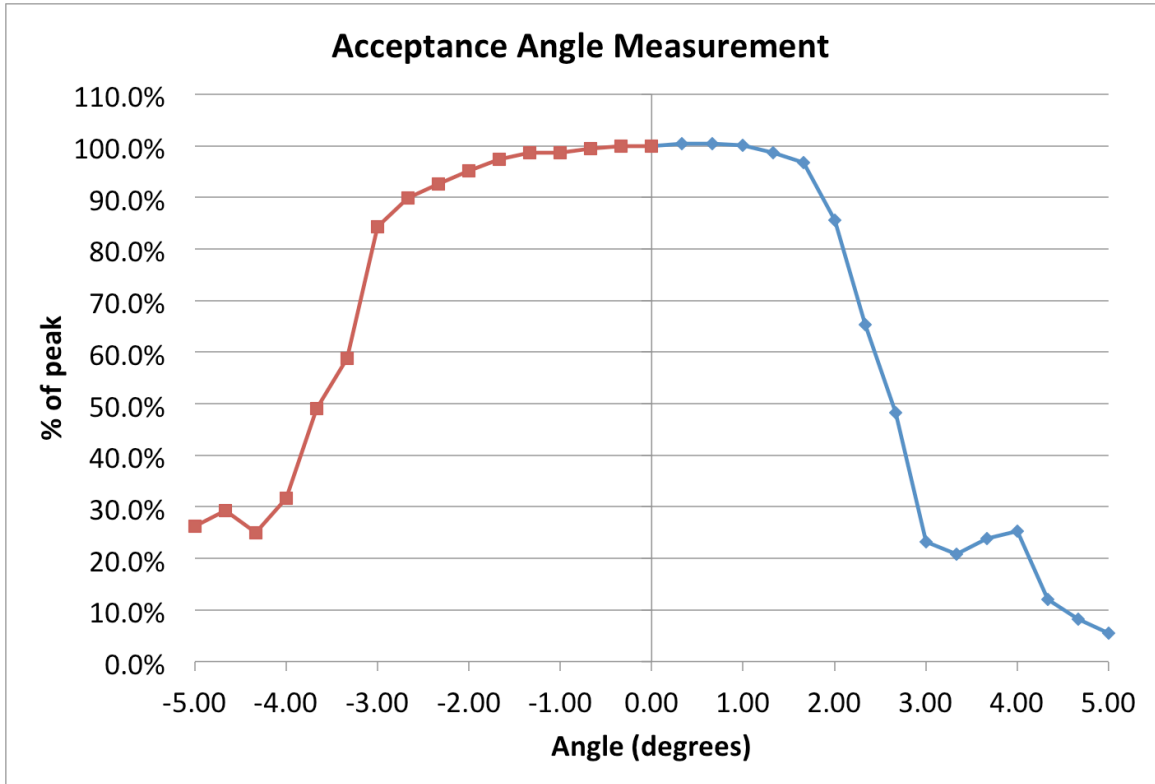


Figure 9 – Acceptance angle measurements from 9/12/14

#### 4.2 Indoor Measurements

In addition to the outdoor acceptance angle measurements, we also used two separate methods to help characterize lens arrays using indoor tools. These were necessary to provide more standardized light sources than solar radiation itself, which is heavily affected by the Earth’s atmosphere. The first of these methods used a spectrometer to measure the transmission spectrum of the lens array, i.e. how much power could pass through the array at a given wavelength. The second method was used to qualitatively study the spot diagrams of the lenses, which help give a clue into how well-focused the lenses were and, from that, how small a concentrated cell could be used underneath the lens array. Both of these methods

proved to be invaluable to helping characterize and further design lens arrays to meet our goal.

#### **4.2.1 Spectroscopy and Transmission Spectra**

Because the sun emits light over a complex emission spectrum, it is important to characterize the transmission spectrum of the lens to make sure that the areas of highest transmission also see the highest energy in the atmosphere. In order to measure these effects, we used two different types of indoor equipment: a solar simulator and a spectrometer. These devices allowed us to take measurements that would have been impractical or impossible outside.

##### **4.2.1.1 Spectroscopy Method**

Spectroscopy was performed through the use of spectrometer and solar generator provided by the University of Delaware Institute of Energy Conversion.

The design of the spectrometer is fairly simple: inside the spectrometer are a number of light emitters, each designed to be able to output at various wavelengths. Through the use of a computer running the spectrometer, a user can define a spectrum and step size over which the spectrometer will emit light at each designated wavelength, pass it through the device being tested, and collect light at the other end. Light collection is performed via an integrating sphere, which is a spherical aperture with highly reflective coating inside. The integrating sphere has a number of ports which can be blocked with similarly-reflective plugs or allowed to

shine light so as to facilitate three different forms of measurement, as illustrated below:

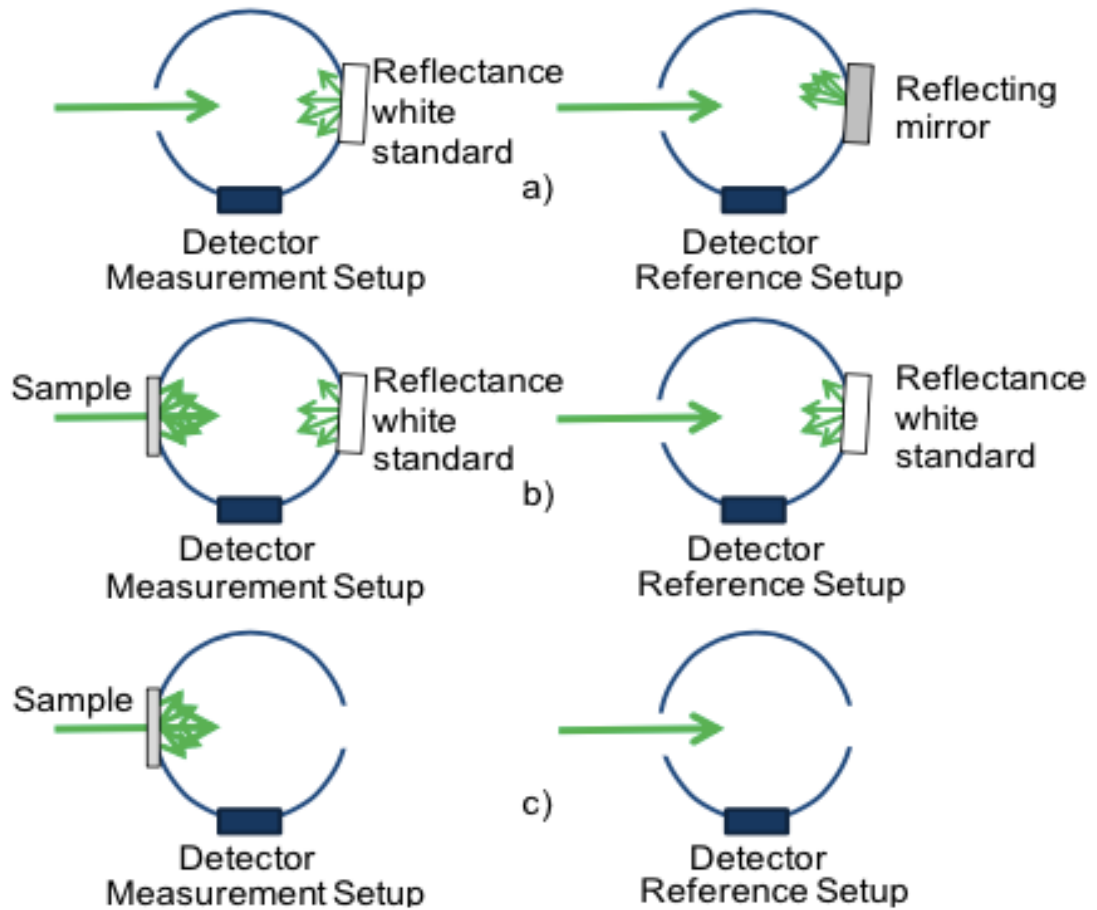


Figure 10 – Integrating sphere setups<sup>20</sup>

It is worth noting that the spectrometer has a critical shortcoming. Because multiple lamps are required to cover the full wavelength spectrum of measurement possibilities, there exist certain points at which one lamp must switch off while other lamps switch on. As one lamp warms up while another cools down, the spectrometer fails to properly mitigate the intensity fluctuations and thus produces data too heavily influenced by noise to provide meaningful data. Fortunately, these errors exist over only a tiny fraction of the spectrum. In order to compensate for

this, all data collected by the spectrometer were analyzed by hand for these error points, and the erroneous data were replaced with linearly interpolated estimates based on the correct data points on either side. While obviously not 100% accurate to the lens array's true response at those wavelengths, this provides something close to the correct data thanks to local linearity and the actual error introduced by this method is negligible.

As detailed in G. Agrawal's paper "Performance Characterization of a Small Form-Factor 100X Micro-Optic Concentrator", each setup is performed both without the sample to serve as a reference as well as with the sample to take actual measurements. This allows us to compensate for certain variables we otherwise would be ignorant to, such as atmospheric conditions in the room and the temperature of the emitting lamps. As shown by Agrawal, the percentage transmission for each of these three steps is given by:

$$\begin{aligned} \%_{3a} &= \frac{P_{in} \eta_{r-diff}}{P_{in}} \\ \%_{3b} &= \frac{P_{in} T_{lens} (n_{lens-r-diff} \eta_{r-diff} + 1 - n_{lens-r-diff})}{P_{in} n_{r-diff}} \\ \%_{3c} &= \frac{P_{in} T_{lens} (1 - n_{lens-r-diff})}{P_{in} n_{r-diff}} \end{aligned}$$

In these expressions,  $P_{in}$  is the incident power,  $\eta_{r-diff}$  is the fraction of light reflected from the diffuser that is detected,  $n_{lens-r-diff}$  is the fraction of transmitted light from the microlens array incident on the rear diffuser, and  $T_{lens}$  is the bulk transmission of

the lens array. Using these equations and the measured results, we could solve for the bulk transmission of the lens array, which is the transmission spectrum.

In order to validate these results, we also tested all lens arrays with a solar simulator. Like the spectrometer, a solar simulator is designed with a certain number of lamps with different emission characteristics, but instead of being designed to output at individual wavelengths, the emission spectrum from the simulator is nearly identical to that output by the sun itself. This allows us to test a physical device under real-world conditions without having to account for errors introduced by the atmosphere, which in turn allows us to find a correction factor for the bulk transmission obtained via spectroscopy. As detailed by Agrawal, the correction factor can be calculated from the solar simulator data via:

$$N = \frac{I_{WithModule}}{I_{WithoutModule}} \frac{\sum_{\lambda} \frac{P_{\lambda} Q E_{\lambda}}{E_{\lambda}}}{\sum_{\lambda} \frac{P_{\lambda} T_{\lambda} Q E_{\lambda}}{E_{\lambda}}}$$

In this formula,  $I_{WithModule}$  and  $I_{WithoutModule}$  are the measured photocurrents with and without the module, respectively,  $\lambda$  is a given wavelength,  $P_{\lambda}$  is the energy at that wavelength as given by the AM1.5G solar data,  $Q E_{\lambda}$  is the quantum efficiency of the photodetector at that wavelength,  $E_{\lambda}$  is the photon energy for a photon of that wavelength (given by Planck's equation  $E_{\lambda} = h\lambda$ ),  $T_{\lambda}$  is the transmission of the module obtained from the spectroscopy measurements, and  $N$  is the correction factor. Like the spectrometer, the solar simulator also suffers from issues at certain

wavelengths due to effects related to the internal lamps, but these problems were compensated for the same way as we did for the spectrometer.

#### **4.2.1.2 Spectroscopy Results**

The best module as measured by spectroscopic methods was found to be the same module as the one verified by the outdoor measurements. Spectroscopic measurements of this module were performed on September 25, 2014 on-site at the Institute of Energy Conversion at the University of Delaware's main campus. Both transmission and reflection were measured, with absorption being calculated from these data via the simple equation  $A = 1 - T - R$ . The highest transmission was found to occur at a wavelength of  $\sim 530\text{nm}$ , at 91.7% transmission. There exists a notable absorption feature in the approximate range of 1600-1800nm wavelengths; this is believed to be a function of the polycarbonate used to manufacture the lens array. Fortunately, reflection remains mostly constant over the entire measured spectrum of 300nm-2000nm, with a peak value of approximately 7.7% reflection and a minimum value of approximately 4.9% reflection. This data was captured with the spectrometer as described in section 4.2.1.1 and adjusted with solar simulator data to better match reality.

The full chart of measured reflectance, absorption, and transmission is reproduced in Figure 11:

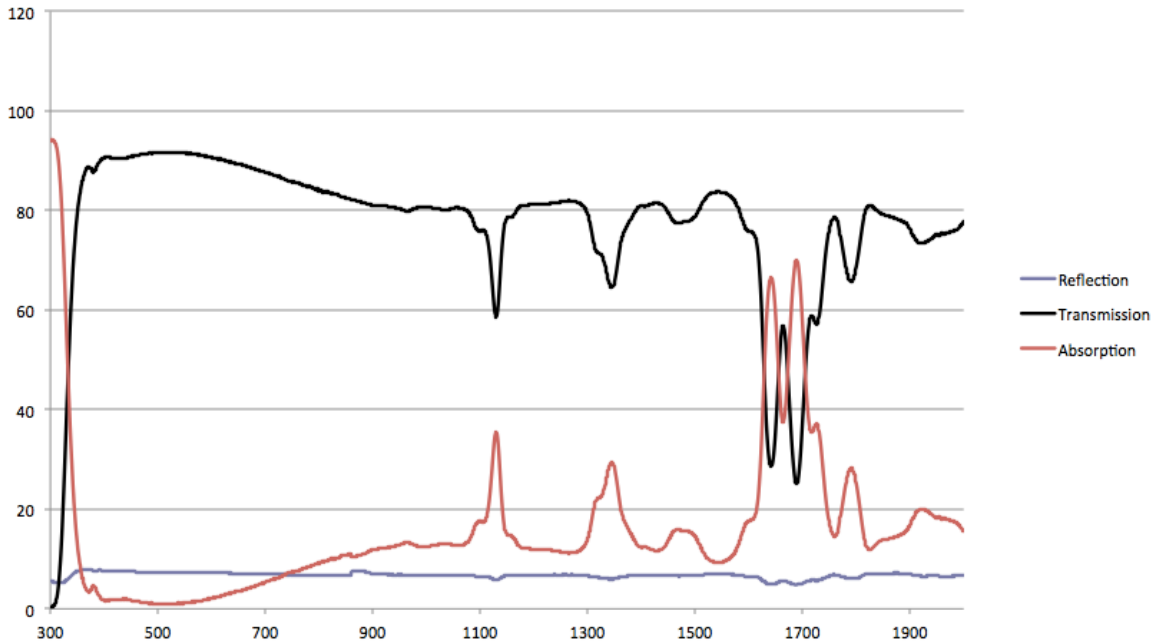


Figure 11 – Absorption, transmission, and reflection percentages for the module tested on 9/25/14

#### 4.2.2 Spot Diagrams

The usage of so-called *spot diagrams* was invaluable to helping characterize the focus characteristics of our modules. These measurements were performed in our laboratory in Evans Hall at the University of Delaware main campus.

A spot diagram is a graphical representation of the focus characteristics of an optical device. Using a spot diagram, we can see where on the geometry of the module light focuses (or “*over-focuses*” into a so-called *hot spot*) as well as locations where light diverges into *cool spots*. While we had no way to quantitatively describe the spot diagram of our lens arrays, these qualitative experiments ultimately proved to be invaluable to helping understand the behavior of each generation of module.

#### **4.2.2.1 Spot Diagram Method**

To perform these experiments, we used a standard vibration-isolation optics table and a number of optical stages in a darkroom. The module to be tested was put in the center of the optical table elevated a few inches off of the surface with a stage. On one side of the table we set up a fiber optic light emitter capable of tight control over the emission intensity. The choice of a fiber optic light source over other kinds of optical emitters was due to the collimated nature of the light output from the fiber: we wanted light that was as close to traveling along the optical axis as possible so as to minimize effects from diffuse lighting. On the other side of the module we attached a standard consumer digital camera to an optical stage in a direct line from the fiber optics. Often, this alignment was done with the aid of an experimental laser in order to ensure a direct linear path for light to travel from the optical fiber, through the module, and into the lens of the camera. From here we adjusted the light levels and took photographs of the light pattern on the module in order to help better understand how light focused coming out of the lens array. On occasion these photographs would also be taken with an additional optical filter between the fiber optic and the lens array. These filters are carefully designed to not affect the optical path of light transmitting through them, but instead to remove some given percentage of energy of the incident beam. This allowed us to have tighter control over the amount of light seen by the lens array than just the fiber optic alone would have given us.

Unfortunately, it is not possible to perform this measurement with the same lens arrays as used for all of the other experiments. This is because in order to avoid visual artifacts from the camera being misfocused on the incoming light, the camera needed a surface to focus upon. As a result, for each generation of lens array we actually had two different arrays: one built as expected for usage in the other forms of experiment, and one created with one planar surface heavily abraded. This created a plane of scattered light, which was enough for the digital camera to focus on the lens array instead of either the fiber optic cable or, worse, nothing at all. Naturally, this abrasion would cause heavy distortion in transmission/absorption/reflectance or acceptance angle measurements, but because the spot diagram experiments were performed for better qualitative understanding of the lens arrays this proved to be not a large issue. There also exists the fact that due to manufacturing defects and errors, there are more physical differences between the abraded and non-abraded lens arrays of the same generation than a single abraded surface, but again these effects should be largely negligible since the spot diagram experiments were performed for qualitative results, not quantitative.

#### **4.2.2.2 Spot Diagram Results**

Unlike for the other experiments described above, there is not an easily-definable “best” module tested since all spot diagrams are merely qualitative descriptors of the lens arrays they represent. For this reason, we will continue to analyze the same module as before so as to provide consistency in these analysis examples.

The clearest spot diagrams for this module were photographed with a 50% transmission optical filter between the optical fiber and the lens array itself. The spot diagram reveals that near the center of the lens array, light is well-focused by the lenses to a small target area as desired. Further away from the center of the array, light scatters more and is not as well focused, but this is not terribly surprising as light further in the  $xy$ -plane from the light source is traveling at an angle and thus strikes the lens array at an angle as diffuse light. Nevertheless, we still see some focusing effects on these further lenses as desired. On a few lenses, notably ones above the central lens, there are notable hotspots produced by the light which appear as bright white dots. These are believed to be due to fabrication flaws; nevertheless, an actual consumer-focused version of the module would necessarily need to have tighter manufacturing controls since hot spots on an unusually bright day could lead to damage to the solar cell underneath the lens array.

The spot diagram for this module as well as a natural-light photograph are reproduced in Figure 12.

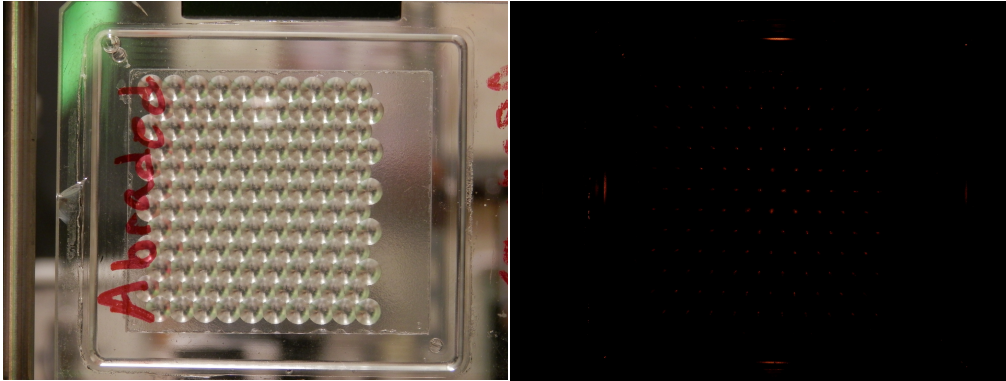


Figure 12 – Spot diagram example: (left) natural light photograph of abraded lens array, (right) spot diagram of the lens array

### 4.3 Analysis of Data

From the data collected and analyzed, we can isolate a few trends in the lens arrays tested.

The first notable trend is that, for the most part, the lens array worked as anticipated. Light striking the lens array at normal incidence was well-focused, and light striking the array at an angle was less tightly focused. The acceptance angle of the lens array was found to be multiple degrees in width as per the design goals, significantly more than the acceptance angle of most high-concentration photovoltaic cells. These two facts combined means that, in the configuration shown in figure 1, we should expect an increased amount of light collected by the photovoltaic cells compared to a CPV setup without our lens array.

A second notable trend is the effect that the physical characteristics of both the material itself and the lens array had on the overall result of the experiments. The

absorption features shown in Figure 11 are troubling, especially since they appear to be the product of an inherent absorption of the material itself. Further experiments with otherwise-identical lens arrays composed of different materials would be necessary to see if this absorption feature is reduced or moved to a less-important section of spectrum. We also see a large number of issues caused by manufacturing errors, such as the hot spots viewed on the spot diagram and the non-symmetry of the acceptance angle measurement. Ideally, were this concept to enter a production environment these issues would be largely mitigated by improved machining techniques for the creation of the lens arrays.

Finally, it should be noted that while the generations tested showed improvement over one another, the entire project was unfortunately cut short for funding reasons. I firmly believe that should the project have continued as planned, many of the issues noted could have been mitigated and the overall efficiency of the lens array improved. As it stands, an evaluation of these data shows a promising if incomplete concept.

## Chapter 5

### CONCLUSION AND FUTURE WORK

The photovoltaic cell has come a long way since its first demonstrations of the photoelectric effect in the 1800s<sup>21</sup>. Nevertheless, as society faces the threat of climate change and the dwindling resources of fossil fuels, the necessity is growing to improve photovoltaic cells even more in order to allow us to switch to cleaner, greener energy technologies. The development of high-concentration photovoltaic cells has provided a marked improvement in absorption potential, but at the cost of the loss of diffuse light in the captured energy.

Throughout this paper we have discussed a possible solution to this issue: hybrid solar cells consisting of both high-concentration photovoltaic cells as well as standard photovoltaic cells, sitting underneath a specially-designed lens array created to maximize the efficiency of the cell structure. These lens arrays have been shown to be very promising, allowing collection on par with standard photovoltaic cells with plenty of room for improvement.

The work performed has validated the basic properties of the micro-lenses as solar concentrating elements. Should the project be continued there exist a few definite targets worth examining:

1. It has been seen that there exist large absorption features on the transmission spectrum of the lens array. It has been hypothesized that this is a function of the polycarbonate material used for the lens array, but without

further experiments this cannot be proven. Additional lens arrays made of competing materials may help mitigate these features.

2. Build quality of the lens arrays must be improved and made more consistent if the arrays are ever to enter a consumer environment. Even small defects on an individual lens can dramatically change the absorbed light on the solar cell underneath the lens, and in some cases could actually cause damage to the cells under unusually bright conditions.
3. Further iteration on lens arrays is necessary. While later generations of arrays showed improvement over their ancestors, they have not been shown to yet be sufficiently more efficient than a standard photovoltaic cell setup to justify the increased cost of more complicated cells and lens arrays.

It is my firm belief that this concept has been shown to be valid and workable, if in need of more work. Should the concept be considered for reevaluation at a later date, the work demonstrated here should provide a solid basis and examination of the viability of the idea and directions to go.

---

## REFERENCES

- <sup>1</sup> "Enterprise and Electrolysis..." Royal Society of Chemistry. Web. 23 Oct. 2015.
- <sup>2</sup> Thornton, Stephen T., and Andrew F. Rex. *Modern Physics for Scientists and Engineers*. 3rd ed. Belmont, CA: Thomson, Brooks/Cole, 2006. 4. Print.
- <sup>3</sup> *Ibid.*, 108
- <sup>4</sup> Saleh, Bahaa E. A., and Malvin Carl Teich. *Fundamentals of Photonics*. 2nd ed. Hoboken, N.J.: Wiley-Interscience, 2007. 446. Print.
- <sup>5</sup> <http://rredc.nrel.gov/solar/spectra/am1.5/>
- <sup>6</sup> "Current Status of Concentrator Photovoltaic (CPV) Technology." Fraunhofer ISE, National Renewable Energy Laboratory. Web. 21 Oct. 2015. <  
<https://www.ise.fraunhofer.de/en/publications/veroeffentlichungen-pdf-dateien-en/studien-und-konzeptpapiere/current-status-of-concentrator-photovoltaic-cpv-technology.pdf>>.
- <sup>7</sup> "Technology » Arzon Solar." Arzon Solar. Web. 21 Oct. 2015.
- <sup>8</sup> M. W. Haney, T. Gu, and G. Agrawal, "Hybrid Micro-scale CPV/PV Architecture"
- <sup>9</sup> N. Yamada, T. Ijiri, W. Goto, K. Okamoto, K. Dobashi, and T. Shiobara, "Development of Silicone-Encapsulated CPV Module Based on LED Package Technology"
- <sup>10</sup> *Ibid.*
- <sup>11</sup> Saleh, Bahaa E. A., and Malvin Carl Teich. *Fundamentals of Photonics*. 2nd ed. Hoboken, N.J.: Wiley-Interscience, 2007. 55.
- <sup>12</sup> G. N. Nielson, M. Okandon, J. L. Cruz-Campa, A. L. Lantine, W. C. Sweatt, V. P. Gupta, J. S. Nielson, "Levaraging scale effects to create next-generation photovoltaic systems through micro- and nanotechnologies", *Proc. SPIE 837317-1*
- <sup>13</sup> See #2
- <sup>14</sup> G. N. Nielson, M. Okandon, J. L. Cruz-Campa, A. L. Lantine, W.C. Sweatt, B. H. Jared, P. J. Resnick, B. Kim, B. J. Anderson, V. P. Gupta, A. Tauke-Pedretti, J. G. Cederberg, T. Gu, M. W. Haney, S. M. Paap, C. A. Sanchez, C. Nordquist, M. P. Saavedra, M. Balance, J. Nguyen, C. Alford, J. S. Nielson, "216 Cell Microconcentrator Module with Moderate Concentration,  $\pm 4^\circ$  Acceptance Angle, and 13.3 mm Focal Length"
- <sup>15</sup> G. Agrawal, T. Gu, M. W. Haney, "Performance Characterization of a Small Form-Factor 100X Micro-Optic Concentrator"
- <sup>16</sup> *Ibid.*
- <sup>17</sup> *Ibid.*
- <sup>18</sup> *Ibid.*
- <sup>19</sup> <http://optics.synopsys.com/lighttools/>
- <sup>20</sup> See #7
- <sup>21</sup> Thornton, Stephen T., and Andrew F. Rex. *Modern Physics for Scientists and Engineers*. 3rd ed. Belmont, CA: Thomson, Brooks/Cole, 2006. 404. Print.